Protein Science (1999), *8*:2019–2026. Cambridge University Press. Printed in the USA.

Structure and function of the N-linked glycans of HBP/CAP37/azurocidin: Crystal structure determination and biological characterization of nonglycosylated HBP

L.F. IVERSEN,[1] J.S. KASTRUP,[2] S.E. BJØRN,[1] F.C. WIBERG,[1] I.K. LARSEN,[2] H.J. FLODGAARD,[1] AND P.B. RASMUSSEN[1]

[1]Novo Nordisk A/S, Novo Allé, DK-2880 Bagsvaerd, Denmark
[2]Department of Medicinal Chemistry, Royal Danish School of Pharmacy, Universitetsparken 2, DK-2100 Copenhagen, Denmark

(RECEIVED May 7, 1999; ACCEPTED July 29, 1999)

Abstract

The three N-glycosylation sites of human heparin binding protein (HBP) have been mutated to produce a nonglycosylated HBP (ng-HBP) mutant. ng-HBP has been crystallized and tested for biological activity. Complete X-ray data have been collected to 2.1 Å resolution, and the structure has been fully refined to an *R*-factor of 18.4% (R_{free} 27.7%). The ng-HBP structure reveals that neither the secondary nor tertiary structure have changed due to the removal of the glycosylation, as compared to the previously determined glycosylated HBP structure. Although the primary events in N-linked glycosylation occurs concomitant with polypeptide synthesis and therefore possesses the ability to influence early events in protein folding, we see no evidence of glycosylation influencing the structure of the protein. The root-mean-square deviation between the superimposed structures was 0.24 Å (on Cα atoms), and only minor local structural differences are observed. Also, the overall stability of the protein seems to be unaffected by glycosylation, as judged by the *B*-factors derived from the two X-ray structures. The flexibility of a glycan site may be determined by the local polypeptide sequence and structure rather than the glycan itself. The biological in vitro activity assay data show that ng-HBP, contrary to glycosylated HBP, mediates only a very limited stimulation of the lipopolysaccharide induced cytokine release from human monocytes. In animal models of fecal peritonitis, glycosylated HBP treatment rescues mice from and an otherwise lethal injury. It appears that ng-HBP have significant effect on survival, and it can be concluded that ng-HBP can stimulate the host defence machinery albeit to a lesser extent than glycosylated HBP.

Keywords: azurocidin; CAP37; CLP; HBP; monocyte; N-linked glycans; protein crystallography; structure function

The function of glycanes covalent attached to proteins has been discussed in past years, especially the biological function of glycanes and how glycanes affect the folding process of the nascent polypeptide chain, and in turn the overall fold of the protein (Cumming, 1992; Lis & Sharon, 1993; O'Connor & Imperiali, 1996; Rudd & Dwek, 1997). Although asparagine-linked (N-linked) glycosylation is observed frequently on secreted proteins, as the human heparin binding protein (HBP), the role of the glycans are not always evident. It has been reported that glycans can stabilize the protein structure (Ingham et al., 1995; Mer et al., 1996), alter the biological properties of the protein (Kaushal et al., 1994; Lu et al., 1995; Chuang & Morrison, 1997), and induce pharmacokinetic changes depending on sialylation or total lack of glycosylation (Thotakura et al., 1991; Sareneva et al., 1993). Glycane induced folding and structure alteration studies (β-turn/hairpin induction) are in many cases performed with short peptides (O'Connor & Imperiali, 1996; Rudd & Dwek, 1997), and it is questionable whether these observations comply with full length proteins.

Three N-linked glycosylation sites have been identified in the human HBP sequence (Asn100, Asn114, and Asn145). A glycosylation site frequently accommodates different glycanes. The microheterogeneity creates discrete subsets or glycoforms of the glycoprotein that can have different physical and biochemical properties (Cumming, 1992; Lis & Sharon, 1993). HBP purified from human blood shows differential glycosylation as the reported molecular mass from different laboratories varies from 28 to 39 kDa (Pereira, 1995). Also, HBP produced in insect cells shows microheterogeneity. It has been reported that the dominant glycoform of insect cell expressed HBP holds two $GlcNac_2Man_3$(Fuc) units and one $GlcNac_2Man_3$ unit, assuming that all three sites are occupied (Rasmussen et al., 1996; Karlsen et al., 1998). The predominant

Reprint requests to: Lars Fogh Iversen, Novo Nordisk A/S, Novo Allé, DK-2880 Bagsvaerd, Denmark; e-mail: lfiv@novo.dk.

Abbreviations: CLP, cecal ligation and puncture; Fuc, fucose; GlcNac, N-acetylglycosamine; HBP, heparin binding protein; HEPES, *N*-(2-hydroxyethyl)piperazine-*N*′-2-ethanesulfonic acid; LPS, lipopolysaccharide; Man, mannose; ng-HBP, nonglycosylated HBP; PCR, polymerase chain reaction; PDB, Protein Data Bank; PKC, protein kinase C; RMSD, root-mean-square deviation; SDS-PAGE, sodium dodecyl sulfate–polyacrylamide gel electrophoresis.

species of N-linked glycans observed from insect cell expression have so far been hexasaccharides with and without a fucose subunit linked to the proximal N-acetyl glucosamine residue (Grabenhorst et al., 1993; Manneberg et al., 1994).

Glycosylated HBP purified from human blood or produced by insect cells (native recombinant HBP) has in recent years been used to clarify the biological functions of HBP. HBP seems to be involved in host defense against infections by acting as chemoattractant for monocytes, T-cells, and K-cells and induces longevity and differentiation of monocytes toward a macrophage phenotype (Flodgaard et al., 1991; Ostergaard & Flodgaard, 1992). Endothelial cells and fibroblasts in monolayers are stimulated by HBP to detach and aggregate (Ostergaard & Flodgaard, 1992). The lipopolysaccharide (LPS) and lipid A binding capacity of HBP (Pereira et al., 1993; Flodgaard & Göricke, 1994) seems to be related to HBP's antibactericidal activity (Shafer et al., 1984; Pereira et al., 1993; Iversen et al., 1997). Upon binding to the lipid A component of LPS, found in the outer membrane of Gram-negative bacteria, HBP might induce leakage of the bacterial membrane (Iversen et al., 1997). The LPS binding might be part of a LPS monocyte presentation mechanism, since monocyte cytokine release is strongly dependent of both the presence of HBP and LPS (Rasmussen et al., 1996). Also, the possibility exists that HBP is capable of priming monocytes to enhance the response when challenged with LPS (Rasmussen et al., 1996; Heinzelmann et al., 1998).

HBP is an inactive serine protease homologue with highest primary sequence identity to neutrophil elastase and proteinase 3 (Flodgaard et al., 1991). The crystal structure of human native recombinant HBP has confirmed the homology to serine proteases by having the same core structure as these enzymes (Iversen et al., 1997; Karlsen et al., 1998). However, a significant different surface charge distribution is found on HBP showing two patches of basic and acidic amino acid residues, respectively (Iversen et al., 1997). Furthermore, in the surface loops, having little or no sequence conservation compared to the serine proteases, a putative lipid A binding site and a putative endothelial cell protein kinase C (PKC) activation site has been identified in the structure (Iversen et al., 1997; Karlsen et al., 1998). The N114 glycosylation site is part of the putative PKC activation site; thus, the glycosylation on HBP might possess the ability to be directly involved in a cellular activation mechanism. Glycosylation sites N100 and N114 are located in the long surface loop, which serves as a domain linker, connecting the two similar domains of HBP, which consist of a closed β-barrel of six antiparallel β-strands. Since neutrophil elastase has one N-glycosylation site in the same domain linker, this glycosylation site might be important for folding of the two domains into the right position with respect to each other. The N145 glycosylation site is situated in β-strand no. eight in the second β-barrel of HBP (Iversen et al., 1997; Karlsen et al., 1998).

By site-directed mutagenesis we have generated a HBP cDNA derivative in which all three N-linked glycosylation sites have been destroyed by three amino acid substitutions. The mutant was produced to investigate the structure and function of nonglycosylated HBP (ng-HBP). The native recombinant HBP and ng-HBP were produced using the same insect cell expression system in order to eliminate structural/functional differences not related to the glycans. To our knowledge, a crystallographic structure determination of a glycosylated and nonglycosylated protein has not been reported in the literature, probably due to the difficulty involved in the crystallization of glycosylated proteins. Here, we present the crystal structure of ng-HBP compared against the structure of native recombinant HBP followed by an assessment of the in vitro and in vivo biological activities of the two HBP forms.

Results

To eliminate a potential N-glycosylation site from a protein, either the Asn or the Ser/Thr residues in the consensus sequence (Asn-Xaa-Ser/Thr) have to be mutated. For unknown reasons it was not possible by site-directed mutagenesis to generate a ng-HBP derivative with the N100Q, N114Q, and N145Q mutations present in the same molecule (data not shown), so the N100Q, N114Q, and T147Y mutant was selected.

A clear decrease in the molecular weight and microheterogeneity of ng-HBP compared to native recombinant HBP is observed from SDS-PAGE gel and MALDI MS analysis (results not shown).

The ng-HBP structure was solved by difference Fourier, using the structure of native recombinant HBP to get initial phases. The mutations N114Q and T147Y were easily identified and built into the $2|F_o| - |F_c|$ and $|F_o| - |F_c|$ electron density maps. However, the side chain of Q100 in the ng-HBP structure is not well defined in the electron density (see Fig. 1). In the Ramachandran plot, no residues are observed in the disallowed regions. V50 is the only residue found in the generously allowed region. Eighty-eight and one-tenth percent of the residues are found in the most favored regions and 11.4% in the additionally allowed regions. Two hundred twenty-one residues of 225 were built (residues 44–47 were not identified in the maps), and 174 water molecules were inserted. For further statistics see Table 1.

Superimposing the Cα atoms of the native recombinant HBP (1.1 Å data) and of ng-HBP the RMSD is 0.24 Å (221 atoms were used in the calculation). No significant backbone or overall structural differences are observed between the two structures (see Fig. 2A). Focusing on the three mutation sites (glycosylation sites), the following differences are observed. Around residue Q100 and Q114 of ng-HBP, only minor differences in hydrogen bonding patterns are observed. The largest structural differences of the three mutation sites are seen around residue Y147 (see Fig. 2B). The bulky side chain of Y147 occupies the space between the R122 and L164 side chains. This side-chain mutation forces the L164 to move approximately 0.4 Å compared to the native recombinant HBP structure, and the side chain of R122 adopts a different conformation in ng-HBP.

The overall protein stability as judged by the average *B*-factors for the ng-HBP and native recombinant HBP structures are within the same range. ng-HBP and native recombinant HBP have similar flexible loops residues and stable core residues. Also, no local significant changes in *B*-factors are observed in the glycosylation site residues or adjacent residues (see Fig. 3).

To assess the biological activity of ng-HBP, it was compared to native recombinant HBP with respect to its ability to enhance, in a dose-dependent manner, the LPS-induced Il-6 release from human monocytes in vitro (Rasmussen et al., 1996). As seen in Figure 4, ng-HBP, in contrary to native recombinant HBP, only mediates a very limited enhancement of the Il-6 release and the dose-dependent relationship, as seen with native recombinant HBP, is not present.

In animal models of fecal peritonitis, native HBP treatment rescues mice from an otherwise lethal injury (Mercer-Jones et al., 1996). To test whether this function was impaired ng-HBP was compared to native recombinant HBP in the Cecal Ligation and Puncture (CLP) model. From Figure 5 it appears that ng-HBP has significant effect on survival, and it can be concluded that ng-HBP

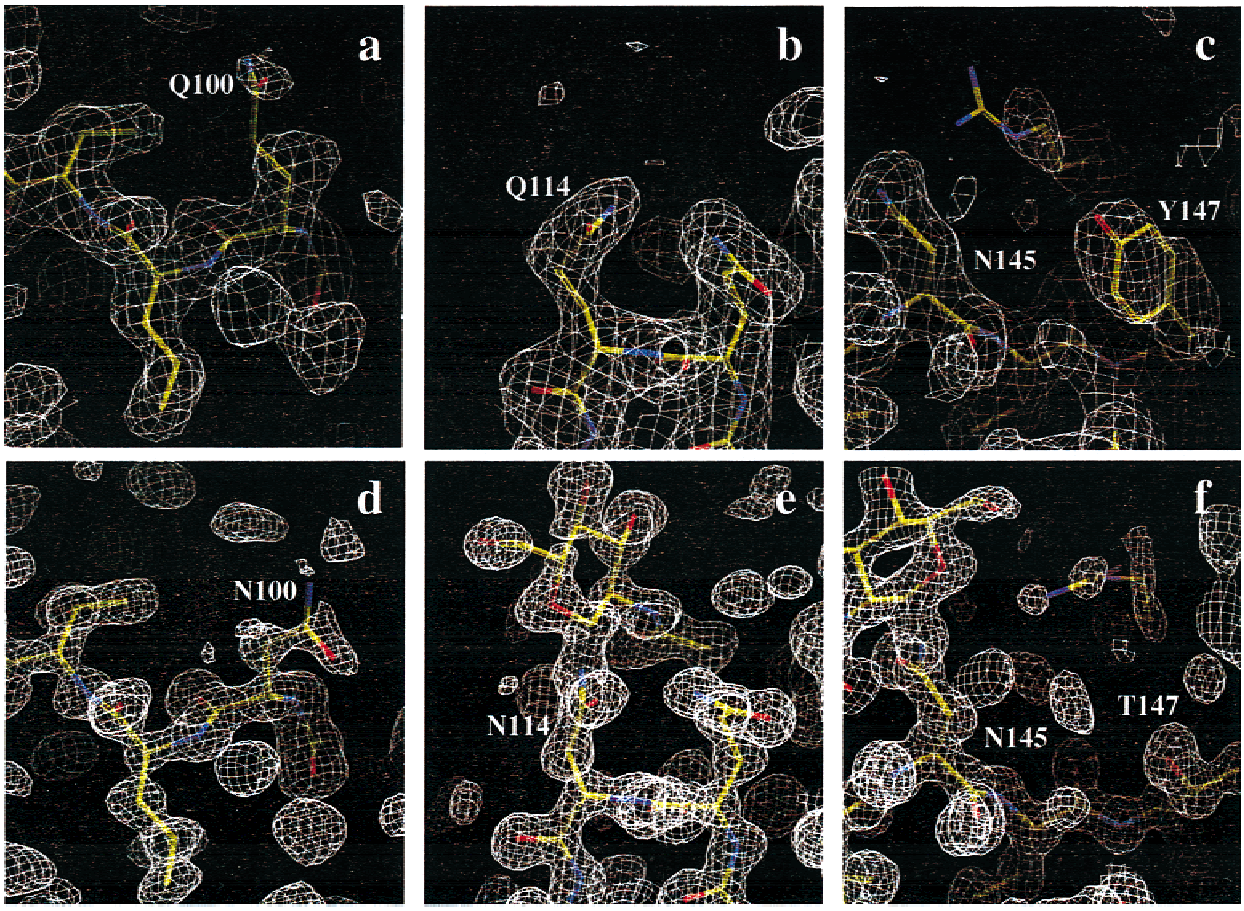

Fig. 1. The electron density maps of the mutated residues in the ng-HBP structure and the native recombinant HBP structure, respectively. The $2|F_o| - |F_c|$ maps contoured at 1σ level are in white and the $|F_o| - |F_c|$ maps contoured at 3σ level are in red. The atoms are colored according to atom types: carbon in yellow, oxygen in red, and nitrogen in blue. **A:** Residue Gln100 of ng-HBP. **B:** Residue Gln114 of ng-HBP. **C:** Residues Asn145, Val146, and Tyr147 of ng-HBP. **D:** Asn100 of native recombinant HBP. **E:** Asn114 of native recombinant HBP. **F:** Asn145 of native recombinant HBP. Figures are made using O (Jones et al., 1991).

can stimulate the host defence machinery albeit to a lesser extent than native recombinant HBP. After seven days the mortality was 9% for native recombinant HBP treated mice, 25% for ng-HBP treated mice, and 47% for untreated (carrier) mice. This corresponds to a fivefold reduction of the mortality for native recombinant HBP treated mice and twofold reduction for the ng-HBP treated mice.

Discussion

The ng-HBP structure has been determined to 2.1 Å resolution and shows that the lack of glycosylation does not affect the fold of the protein. The secondary and tertiary structures of ng-HBP and native recombinant HBP are nearly identical.

The local structural differences observed around Y147 might be caused by either the introduction of the bulky Tyr side chain, the removal of the glycosylation, or a combination of both. The L164 is not in close contact with N145 or with the glycosylation at this site and might only be affected by the Y147 side chain. R122 might have altered their side-chain conformation due to the removal of the glycosylation as well as the side chain (see Fig. 2B). In native recombinant HBP, the R122 side chain is forming a hydrogen bond to an oxygen atom of the proximal GlcNac unit on N145, where as this side chain in ng-HBP is involved in stacking interactions with the Y147 side chain. In the case of HBP, the folding of the protein seems independent of glycosylation.

The *B*-factor plot (Fig. 3) clearly unveils that ng-HBP and native recombinant HBP have the same degree of structural stability. Furthermore, the surface loops to where the glycans are attached are also unaffected by the removal of the glycosylation. This finding is in contrast to previous papers, where glycosylation was reported to stabilize the protein structure (Ingham et al., 1995; Runkel et al., 1998).

The minor structural changes between ng-HBP and native recombinant HBP described in the above are not likely to explain why the in vitro biological activity of ng-HBP, as measured by LPS induced IL-6 release from human monocytes, has been reduced to a minimal level as well as its in vivo effect in the CLP model has been lowered. The putative heparin binding site, the LPS (lipid A) binding site, and PKC activation site (Iversen et al., 1997; Karlsen et al., 1998) are not influenced by the structural differences observed in the area of Y147. Upon complex formation, favorable carbohydrate–carbohydrate interactions between LPS and the glycosylation chains of HBP might have a complex stabilizing effect.

Table 1. *X-ray data statistics*

Statistics of data and refinement	
Space group	P212121
Unit cell parameters	$a = 38.25$, $b = 65.52$, $c = 101.17$ Å
Completeness (20–2.1 Å)	96.7%
Completeness (2.17–2.13 Å)	93.3%
Multiplicity (20–2.1 Å)	3.6
R_{merge} (20–2.1 Å)	8.7%
R_{merge} (2.17–2.13 Å)	27.6%
$\langle I/\sigma(I)\rangle$ (20–2.1 Å)	11.9
$\langle I/\sigma(I)\rangle$ (2.17–2.13 Å)	4.3
Unique reflections	14,365
Atoms in structure	1,853
R-factor[a]	18.4%
R-free[b]	27.7%
RMSDs from idealized geometries	
Bond lengths (Å)	0.016
Bond angles (°)	2.5
Dihedral angles (°)	17.8
Planar groups (Å)	0.012
Bad contacts (Å)	0.016
RMSDs between atoms	
B-factors (all atoms) (Å^2)	3.2

[a]The *R*-factor was calculated using all data from 20 to 2.1 Å.

$$\text{Crystallographic } R\text{-factor} = \sum_{(hkl)} ||F_o| - |F_c|| \Big/ \sum_{(hkl)} |F_o|.$$

[b]$R_{free} = \sum_{(hkl)\in T} ||F_o| - |F_c|| / \sum_{(hkl)\in T} |F_o|$ where T is a test set containing a random of 5% of the observations omitted from the refinement process.

It has been demonstrated that HBP is internalized when given to monocytes (Heinzelmann et al., 1998, 1999). To get internalized, HBP might have to get in contact with an anchoring/docking site on the target cell membrane, and it is possible that the lack of glycosylation on ng-HBP hinders the contact to this site on the membrane. The fact that ng-HBP was almost unable to stimulate the LPS induced Il-6 release in vitro from the monocytes fits with the hypothesis that the internalization of ng-HBP has been impaired. However, the in vivo CLP experiment showed that the ng-HBP possessed the ability to reduce the mortality twofold, thus showing that ng-HBP is still a potent and active molecule, although to a lesser extent than native recombinant HBP.

A 10-fold lowering of biological activity was observed for the nonglycosylated human interferon-β compared to the glycosylated protein (Runkel et al., 1998). It was concluded that the main reason for the lowered activity of nonglycosylated human interferon-β was protein instability due to lack of glycosylation. In the present study, we have demonstrated that protein stability is nearly identical for native recombinant HBP and ng-HBP, and thus cannot account for the diminished biological activity observed for ng-HBP. The discrepancy in biological activity is more likely to be found in other parameters than stability.

The glycan at N100 was not observed in the electron density maps in the native recombinant HBP structure (Iversen et al., 1997; Karlsen et al., 1998). This was believed to be due to the localization of this site at a large water channel spanning through the crystal, leaving plenty of space for the movements of a flexible glycosylation chain. Consistent with this, the side chain of Q100 in the ng-HBP structure is not well defined in the electron density (see Fig. 1), thus, residue 100 retains its side-chain flexibility even in the nonglycosylated state. This indicates that the flexibility of a glycosylation site might be determined by the local polypeptide sequence and structure rather than the glycosylation attached to a certain site. At the two other glycosylation sites where glycosylation could be determined in the native recombinant HBP structure, we find well-defined and stable side chains in the ng-HBP structure. The impact of the flexibility of glycans at different sites on the function of the protein is not known, but it can be speculated that flexible glycosylation is capable of shielding larger protein surface areas (surface charges, hydrophobic patches, and sensitive loops, see Fig. 6) while stable glycosylation is more likely to be involved in specific interactions at the molecular level.

In conclusion, despite the fact that neither protein fold, structure, nor stability appear to be influenced by the removal of the glycosylation from HBP, the biological activity with respect to in vitro stimulation of the LPS induced Il-6 release from monocytes is severely affected. However, ng-HBP was demonstrated to be an active molecule in vivo with a significant twofold lowering of the mortality in the CLP model.

Materials and methods

HBP mutagenesis

To generate a cDNA encoding, the ng-HBP derivative the HBP cDNA in pSX559 (Rasmussen et al., 1996) was altered by site-directed PCR mutagenesis. First, the asparagine in position 100 was changed to a glutamine residue: Using Pfu polymerase (Stratagene, La Jolla, California), two PCR reactions were performed with two overlapping primer-sets [PBRa 247 (5′-CCGGGGATCC GATGACCCGGCTGACAGTCCTGG-3′)/PBRa 302 (5′-GCTGC TGGTGAGCTGGGCCTCACGGTCCAG-3′) and PBRa 301 (5′-CTGGACCGTGAGGCCCAGCTCACCAGCAGC-3′)/PBRa 246 (5′-CCGGGGATCCAACTAGGCTGGCCCCGGTCCCGG-3′) resulting in two fragments of 390 and 396 base pairs, respectively. These two fragments were assembled in a third PCR with the flanking primers PBRa 247 and PBRa 246. The resulting HBP cDNA derivative was inserted into the transfer vector pVL1393 (Invitrogen, San Diego, California) and confirmed by DNA sequencing to have the correct base changes leading to the N100Q shift. Hereafter, by the same procedure, the T147Y substitution was introduced into the HBP N100Q cDNA template by usage of the overlapping primers PBRa 324 (5′-AGGTTCGTCAACGTGT ACGTGACCCCCGAGGAC-3′) and PBRa 325 (5′-GTCCTCGG GGGTCACGTACACGTTGACGAACCT-3′). Finally, the N114Q substitution was introduced into the HBP N100Q, T147Y cDNA template by using the overlapping primers PBRa 303 (5′-CTGCC TCTGCAGCAGGCCACGGTGGAAGCC-3′) and PBRa 304 (5′-GGCTTCCACCGTGGCCTGCTGCAGAGGCAG-3′). Generation of recombinant baculovirus containing the HBP N100Q, N114Q, T147Y cDNA was done as described previously (Rasmussen et al., 1996).

Expression and purification

ng-HBP was expressed and purified as described for the native recombinant HBP protein (Rasmussen et al., 1996).

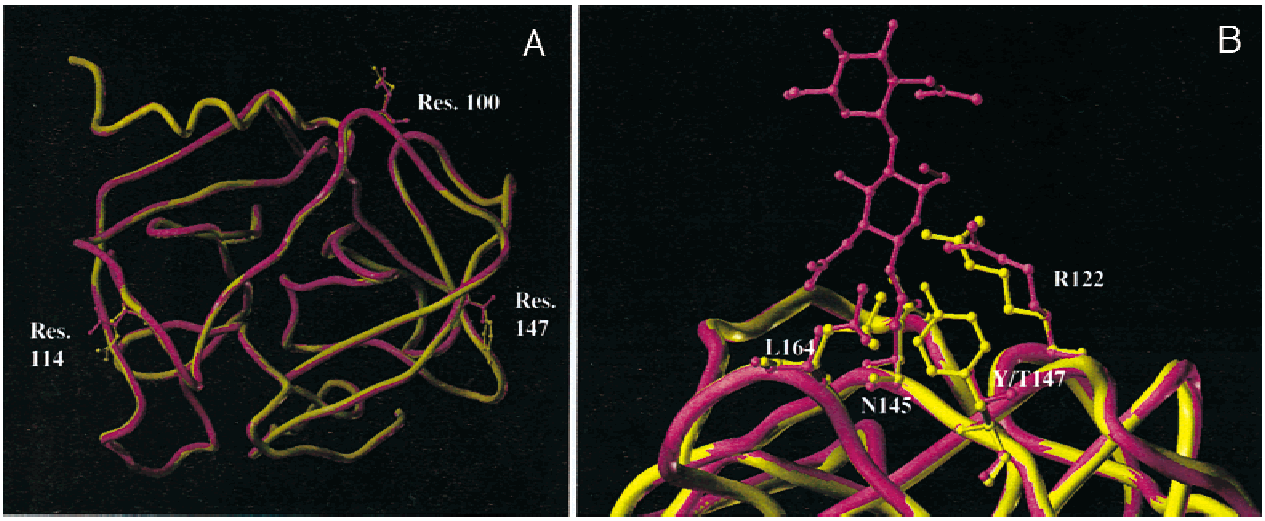

Fig. 2. **A**: The superimposed structures of native recombinant HBP (magenta) and ng-HBP (yellow). The three mutation sites in ng-HBP are labeled. The tube representation was made by the use of Sybyl (Tripos Associate Inc., St. Louis, Missouri). **B**: The superimposed structures of native recombinant HBP (magenta) and ng-HBP (yellow). The area around the Thr147 to Tyr mutation. All the affected residues are shown and labeled. The tube representation was made by the use of Sybyl (Tripos Associate Inc.).

Crystallization

The ng-HBP protein was concentrated to a 5 mg/ml solution in 5 mM HEPES buffer pH 7.8 using a Millipore microconcentrator (Ultrafree-MC 20.000 NMWL filter unit).

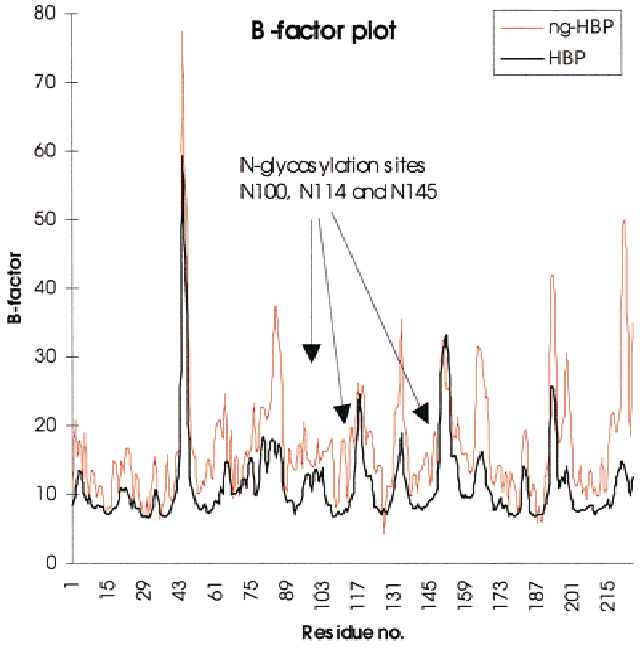

Fig. 3. *B*-factor plot of the ng-HBP and native recombinant HBP structures. The plot was made using the Cα backbone atomic displacement factors (*B*-factors) for each residue for each structure. The native recombinant HBP data were collected at 100 K and to 1.1 Å resolution (isotropic *B*-factor's used). The ng-HBP data were collected at 110 K and to 2.1 Å resolution.

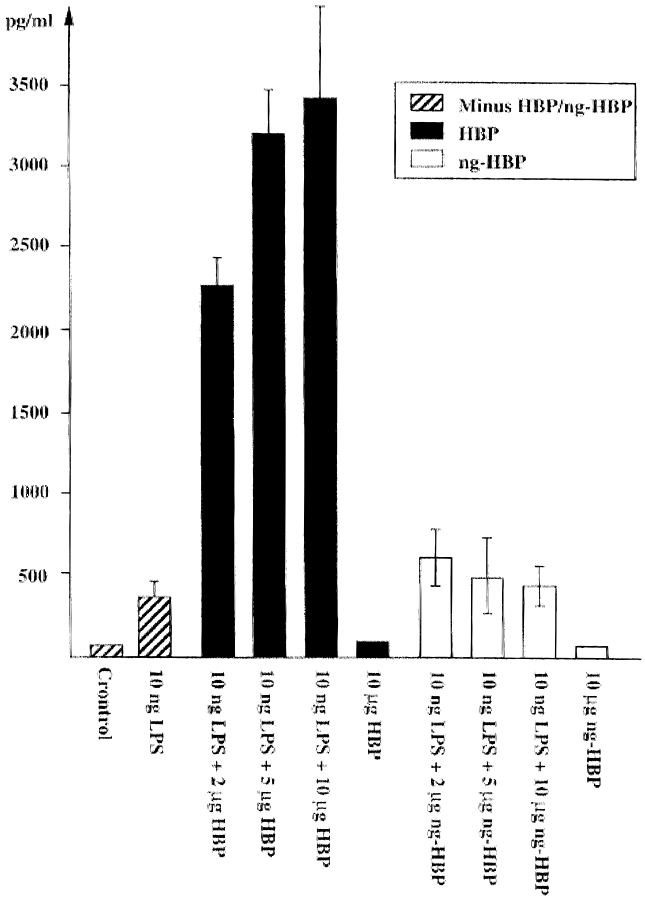

Fig. 4. Il-6-release from human monocytes. The monocytes were cultured in 1 mL of serum-free medium for 24 h in the presence of LPS and/or recombinant native recombinant HBP (HBP)/ng-HBP in the amounts indicated in the figure. The bars are mean values and standard deviations calculated from four separate measurement points.

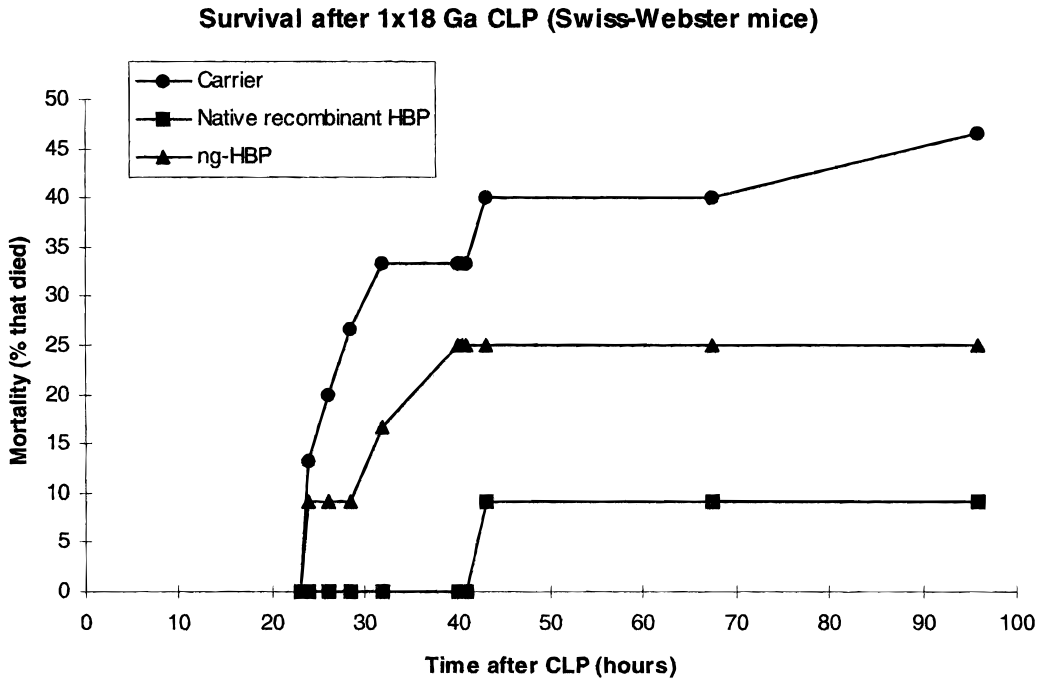

Fig. 5. Mortality following single 18-gauge CLP; $n = 12$ in the native recombinant HBP and ng-HBP groups, and $n = 15$ in the carrier (untreated) group.

Crystallization was done with the hanging-drop vapor-diffusion method using the repeated seeding technique. All experiments were performed at 20 °C with drop sizes of 2 μL protein solution and 2 μL reservoir solution. The reservoir volume was 1 mL. Microseeding with crushed native recombinant HBP microcrystals (Iversen et al., 1996) was performed using 6% ethanol, 5% glycerol, 8 mM $MgSO_4$, and 0.1 M Tris pH 7.2 as reservoir solution. An additional round of microseeding with ng-HBP crystals was performed to dilute any remains of native recombinant HBP protein in the crystals. Macroseeding with ng-HBP crystals was done under similar conditions as microseeding. Crystals grew to maximum size of $0.3 \times 0.3 \times 0.3$ mm within 3–4 days.

Data collection and data processing

One crystal of the size $0.3 \times 0.05 \times 0.05$ mm was used for data collection at cryogenic temperature on the EMBL X11 beamline in Hamburg, using a small Mar image plate detector. Three microliter cryosolution containing 40% glycerol in the above standing crystallization buffer was added to the hanging-drop ~30 s before flash-freezing (110 K) of the crystal. Crystals of the size $0.3 \times 0.3 \times 0.3$ mm could not be used for flash-freezing due to cracks and destruction of the crystals upon freezing. Auto-indexing and data processing were performed with DENZO and SCALEPACK (Otwinowski, 1986) (see Table 1).

Structure solution and refinement

The initial phases for the ng-HBP structure were generated from the native recombinant HBP structure (Iversen et al., 1996, 1997)

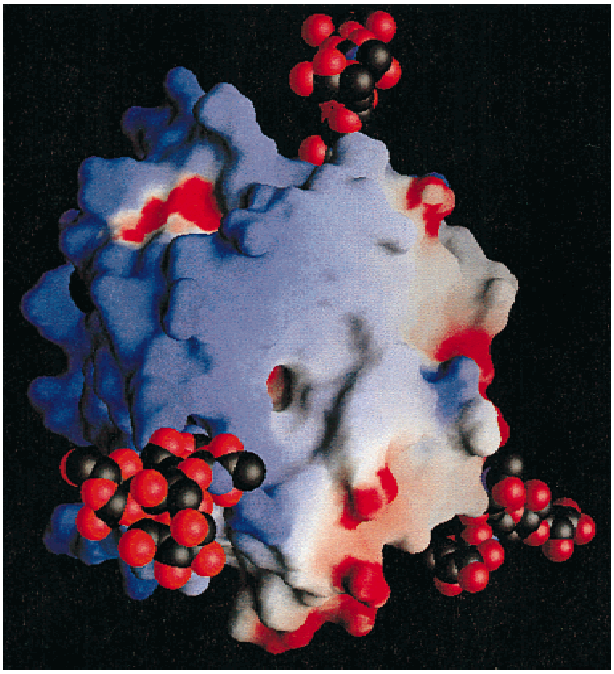

Fig. 6. Glycosylation modeled at all three site. Glycosylation for the native recombinant baculovirus expressed HBP (according to (Rasmussen et al., 1996)) was modeled manually using the program O. The surface electrostatic potential was calculated and rendered by the use of GRASP (Nicholls et al., 1991). Positive potential is colored in blue and negative potential in red. Glycosylation atoms are colored according to atom type: carbon in black, oxygen in red, and nitrogen in blue.

without water molecules and glycosylation chains included (isomorphous cell parameters). Ten cycles of rigid body refinements were performed, followed by 10 cycles of positional refinement and 30 cycles of positional and *B*-factor refinements. The structure was inspected and corrected using the program O (Jones et al., 1991). At this stage the three mutations in the structure were introduced, and the side chains were fitted to the electron density maps. Water molecules were added to the structure after the following criteria: difference Fourier $|F_o| - |F_c|$ peaks should be stronger than 3σ and defined in the $2|F_o| - |F_c|$ electron density maps contoured at 1σ level; the density should be nearly spherical; satisfactory hydrogen bond interactions should be formed to protein atoms or other water molecules; and the *B*-factor for the waters should be less than 50 Å^2. An additional 10 cycles of positional and *B*-factor refinements were performed. All refinements were performed with TNT (Tronrud et al., 1987; Tronrud, 1992). The final *R*-factor was 18.4%. The refinement protocol was monitored by the use of R_{free} (5% of data). For further statistics, see Table 1.

Assay of ng-HBP bioactivity

Human monocytes were isolated and treated as described previously (Rasmussen et al., 1996), with the exception that 1% nonessential amino acids were excluded from the medium.

Cecal ligation and puncture (CLP)

Native recombinant HBP (50 μg), ng-HBP(50 μg), or carrier consisting of phosphated saline buffer pH 7.4 (untreated) (0.2 mL) were given i.p. 24 h prior to single 18-gauge CLP. All mice were Swiss-Webster mice. Through a midline laparotomy incision, the cecum was ligated just below the ileocecal junction with 3-0 slik and was punctured once with an 18-gauge needle. Using gentle pressure on the cecum, a small amount of fecal material was expressed to ensure the patency of the puncture hole. The abdominal incision was closed with nylon suture. No fluid resuscitation was given after CLP. Mice were observed for seven days, after which no mice died.

Acknowledgments

We thank Ms. Inge M. Skæpgaard, Ms. Sannie Kaltoft, and Mr. Brian Rosenberg for technical assistance; Prof. William G. Cheadle and Dr. Jim Peyton (University of Louisville) for kindly conducting the CLP experiments. We thank the European Union for support of the work at EMBL Hamburg through the HCMP to Large Installations Project, contract no. CHGE-CT93-0040. This study was supported in part by The Danish Research Academy, The Dansync centre for Synchrotron Radiation, and PharmaBiotec.

References

Chuang PD, Morrison SL. 1997. Elimination of N-linked glycosylation sites from the human IgA1 constant region. *J Immunology 158*:724–732.

Cumming DA. 1992. Physiological relevance of protein glycosylation. *Develop Biol Standard 76*:83–94.

Flodgaard H, Göricke C. 1994. Lipopolysaccharide binding and monocyte chemotaxis are independent functions by HBP, a neutrophil granule-derived cationic protein. *J Cell Biochem Suppl 18A*. Abstract E505.

Flodgaard HJ, Ostergaard E, Bayne S, Svendsen A, Thomsen J, Engels M, Wollmer A. 1991. Covalent structure of two novel neutrophile leucocyte-derived proteins of porcine and human origin. Neutrophile elastase homologues with strong monocyte and fibroblast chemotactic activities. *Eur J Biochem 197*:535–547.

Grabenhorst E, Hofer B, Nimtz M, Jager V, Conradt HS. 1993. Biosynthesis and secretion of human interleukin 2 glycoprotein variants from baculovirus-infected Sf21 cells. Characterization of polypeptides and posttranslational modifications. *Eur J Biochem 215*:189–197.

Heinzelmann M, Mercer-Jones MA, Flodgaard H, Miller FN. 1998. Heparin-Binding Protein (CAP37) is internalized in monocytes and increases LPS-induced monocyte activation. *J Immunology 160*:5530–5536.

Heinzelmann M, Platz A, Flodgaard H, Polk HC Jr, Miller FN. 1999. Endocytosis of heparin-binding protein (CAP37) is essential for the enhancement of LPS-induced TNF-a production in human monocytes. *J Immunology 162*:4240–4245.

Ingham K, Brew SA, Novokhatny VV. 1995. Influence of carbohydrate on structure, stability and function of gelatin-binding fragments of fibronectin. *Archives Biochem and Biophys 316*:235–240.

Iversen LF, Kastrup JS, Bjorn SE, Rasmussen PB, Wiberg FC, Flodgaard HJ, Larsen IK. 1997. Structure of HBP, a multifunctional protein with a serine protease fold. *Nature Struct Biol 4*:265–268.

Iversen LF, Kastrup JS, Larsen IK, Bjorn SE, Rasmussen PB, Wiberg FC, Flodgaard HJ. 1996. Crystallization and molecular replacement solution of human heparin binding protein. *Acta Cryst D 52*:1222–1223.

Jones TA, Zou JY, Cowan SW, Kjeldgaard M. 1991. Improved methods for building protein molecules in electron density maps and the location of errors in these models. *Acta Cryst A 47*:110–119.

Karlsen S, Iversen LF, Larsen IK, Flodgaard HJ, Kastrup JS. 1998. Atomic resolution structure of human HBP/CAP37/azurocidin. *Acta Cryst D 54*: 598–609.

Kaushal S, Ridge KD, Khorana HG. 1994. Structure and function in rhodopsis: The role of aspargine-linked glycosylation. *Biochemistry 91*:4024–4028.

Lis H, Sharon N. 1993. Protein glycosylation. Structural and functional aspects. *Eur J Biochem 218*:1–27.

Lu HS, Chang D, Philo JS, Zhang K, Narhi LO, Liu N, Zhang M, Sun J, Wen J, Yanagihara D, et al. 1995. Studies on the structure and function of glycosylated and nonglycosylated neu differentiation factors. *J Biol Chem 270*:4784–4791.

Manneberg M, Friedlein A, Kurth H, Lahm HW, Fountoulakis M. 1994. Structural analysis and localization of the carbohydrate moieties of a soluble human interferon gamma receptor produced in baculovirus-infected insect cells. *Protein Sci 3*:30–38.

Mer G, Hietter H, Lefevre J. 1996. Stabilization of proteins by glycosylation examined by NMR analysis of a fucosylated proteinase inhibitor. *Nature Struct Biol 3*:45–53.

Mercer-Jones MA, Hadjiminas DJ, Heinzelmann M, Peyton JC, Cook M, Cheadle WG. 1996. Monocyte recruitment increases survival in fecal peritonitis. *Surgical Forum 37*:105–108.

Nicholls A, Sharp KA, Honig B. 1991. Protein folding and association: Insights from the interfacial and thermodynamic properties of hydrocarbons. *Proteins 11*:281–296.

O'Connor SE, Imperiali B. 1996. Modulation of protein structure and function by aspargine-linked glycosylation. *Chem Biol 3*:803–812.

Ostergaard E, Flodgaard H. 1992. A neutrophil-derived proteolytic inactive elastase homologue (hHBP) mediates reversible contraction of fibroblasts and endothelial cell monolayers and stimulates monocyte survival and thrombospondin secretion. *J Leukoc Biol 51*:316–323.

Otwinowski Z. 1986. *DENZO program: An oscillation data processing program for macromolecular crystallography*. New Haven, CT: Yale University.

Pereira HA. 1995. CAP37, a neutrophil-derived multifunctional inflammatory mediator. *J Leukoc Biol 57*:805–812.

Pereira HA, Erdem I, Pohl J, Spitznagel JK. 1993. Synthetic bactericidal peptide based on CAP37: A 37-kDa human neutrophil granule-associated cationic antimicrobial protein chemotactic for monocytes. *Proc Natl Acad Sci USA 90*:4733–4737.

Rasmussen PB, Bjorn S, Hastrup S, Nielsen PF, Norris K, Thim L, Wiberg FC, Flodgaard H. 1996. Characterization of recombinant human HBP/CAP37/azurocidin. A pleiotropic mediator of inflammation enhancing LPS-induced cytokine release from monocytes. *FEBS Lett 390*:109–112.

Rudd PM, Dwek RA. 1997. Glycosylation: Heterogeneity and the 3D structure of proteins. *Critical Rev Biochem Mol Biol 32*:1–100.

Runkel PM, Meier W, Blake Pepinsky R, Karpusas M, Whitty A, Kimball K, Brickelmaier M, Muldowney C, Jones W, Goelz SE. 1998. Structural and functional differences between glycosylated and non-glycosylated forms of human interferon-β (IFN-β). *Pharmaceutical Res 15*:641–649.

Sareneva T, Cantell K, Pyhãlã L, Pirhonen L, Julkunen I. 1993. Effect of carbohydrates on the pharmacokinetics og human interferon-g. *J Interferon Res 13*:267–269.

Shafer WM, Martin LE, Spitznagel JK. 1984. Cationic antimicrobial proteins isolated from human neutrophil granulocytes in the presence of diisopropyl fluorophosphate. *Infect Immun 45*:29–35.

Thotakura NR, Desai RK, Bates LG, Cole ES, Pratt BM, Weintraub BD. 1991. Biological activity and metabolic clearance of a recombinant human thyrotropin produced in chinese hamster ovary cells. *Endocrinology 128*:341–348.

Tronrud DE. 1992. Conjugate-direction minimization: An improved method for the refinement of macromolecules. *Acta Cryst A 48*:912–916.

Tronrud DE, Ten Eyck LF, Matthews BW. 1987. An efficient general-purpose least-squares refinement program for macromolecular structures. *Acta Cryst A 43*:489–501.